Available online at www.sciencedirect.com

SciVerse ScienceDirect

Ceramics International 39 (2013) 6355–6361

CERAMICS INTERNATIONAL

www.elsevier.com/locate/ceramint

# Densification and characterization of $SiO_2$–$B_2O_3$–CaO–MgO glass/$Al_2O_3$ composites for LTCC application

Xingyu Chen*, Weijun Zhang, Shuxin Bai, Yongguo Du

*Department of Materials Science and Engineering, National University of Defense Technology, Changsha 410073, PR China*

Received 21 November 2012; received in revised form 17 January 2013; accepted 18 January 2013
Available online 29 January 2013

**Abstract**

A glass/ceramic composite using lead-free low melting glass ($SiO_2$–$B_2O_3$–CaO–MgO glass) with $Al_2O_3$ fillers was investigated. X-ray diffraction analysis revealed that the anorthite and cordierite phase appeared in the sintered composites. The dilatometric analysis showed that the onset of shrinkage took place at ~624 °C for all the samples and the onset temperature was independent on the content of glass. The low melting glass significantly promoted densification of the composites and lowered the sintering temperature to ~875 °C. The addition of 50 wt% glass sintered at 875 °C showed $\varepsilon_r$ of 7.3, tan $\delta$ of $1.15 \times 10^{-3}$, TEC of 5.41 ppm/°C, thermal conductivity of 3.56 W/m °C, and flexural strength of 184 MPa. The results showed that the $SiO_2$–$B_2O_3$–CaO–MgO glass/$Al_2O_3$ composites were strong potential candidates for low temperature cofired ceramic substrate applications.


*Keywords:* A. Sintering; C. Dielectric properties; Densification; LTCC

## 1. Introduction

In the past decades, low temperature cofired ceramics (LTCC) substrate and related packaging technology have been extensively studied due to their practical and viable merits such as the utilisation of the low melting point of the highly conductive internal electrode metals (e.g., 961 °C for silver and 1083 °C for copper) and the increment of integration density [1–3]. LTCC substrates commonly combine many layers of ceramic and conductors resulting in multilayer modules and have been developed to achieve the criteria of high signal propagation speed, good reliability, and low cost [1,4,5]. Furthermore, in order to meet the requirement for desired LTCC substrates, the permittivity of the LTCC materials should be lower than that of $Al_2O_3$ (~9.8) to diminish signal propagation delay.

Several low-permittivity dielectric compositions have been reported, including production of glass ceramic and glass/ceramic composites [6]. The starting material used in the glass ceramic approach is a pure glass such as cordierite glass, which densifies first, followed by crystallisation. The physical properties of the resulting composition are controlled by the degree of crystallisation, which can be enhanced by addition of a small amount of crystalline phase which acts as a nucleating agent. For the glass/ceramic approach, the low melting glass acts as a densification flux to enhance densification, and the ceramic fillers act to adjust the physical properties of the resulting composites [1,7,8]. Comparing the two approaches, it is a more general method to add glass frits into the ceramic to attain good electrical properties together with acceptable densification at temperature range of less than 900 °C [1]. Hence, the glass/ceramic approach is also taken in the present study.

Most of the known glasses in the LTCC materials are $ZnO$–$B_2O_3$ [9], BaO–ZnO–$B_2O_3$ [10,11], $Li_2O$–$B_2O_3$–$SiO_2$–CaO–$Al_2O_3$ [12], MgO–$B_2O_3$–$SiO_2$ [13], BaO–$B_2O_3$–$SiO_2$ [13], CaO–$B_2O_3$–$SiO_2$ [14], PbO–$B_2O_3$–$SiO_2$ [10], $SiO_2$–$B_2O_3$–ZnO [10], $B_2O_3$–$La_2O_3$–MgO–$TiO_2$ [15], etc. Normally, the compositions of the low melting glass have typically three or more oxides present. $SiO_2$ and $B_2O_3$ commonly form the network structures of glass [16]. PbO, MgO, CaO, $Na_2O$, $K_2O$, and $Li_2O$ are modifier oxides and

*Corresponding author. Tel./fax: +86 731 84574791.
*E-mail address:* hsingyuchan@gmail.com (X. Chen).

0272-8842/$ - see front matter © 2013 Elsevier Ltd and Techna Group S.r.l. All rights reserved.
http://dx.doi.org/10.1016/j.ceramint.2013.01.061

can be used to tailor the physical properties of glass such as lowering the softening point, increasing the thermal expansion or enhancing the chemical durability [1,16].

In this work, attention was focused on the LTCC system based on lead-free $SiO_2$–$B_2O_3$–CaO–MgO–$Na_2O$–$K_2O$ glass (SBCM glass) and $Al_2O_3$ filler. The effects of the glass on sintering, shrinkage, thermal expansion, thermal conductivity, flexural strength, and dielectric properties were investigated in this work.

## 2. Experimental procedure

### 2.1. Preparation of the glass and composites

The batch of raw materials corresponding to the low melting glass with the composition 25 wt% $SiO_2$, 52 wt% $B_2O_3$, 10 wt% CaO, 10 wt% MgO, 1 wt% $Na_2O$, and 2 wt% $K_2O$ was prepared by melting powders containing appropriate amounts of reagent grade $SiO_2$ (99.9%; Bodi Chemical Co. Ltd., China), $H_3BO_3$ (99.0%; Damao Chemical Reagent Co. Ltd., China), MgO (99.9%; Bodi Chemical Co. Ltd., China), $CaCO_3$ (99.9%; Bodi Chemical Co. Ltd., China), $Na_2CO_3$ (99.9%; Damao Chemical Reagent Co. Ltd., China) and $K_2CO_3$ (99.9%; Damao Chemical Reagent Co. Ltd., China) in an uncovered platinum crucible for 2 h at 1500 °C. The melt was quenched into a water bath to form transparent glass. The quenched glass was ball milled with stabilized zirconia balls for 8 h and the average particle size of milled glass frit was ~3 μm. As a next step, $Al_2O_3$ powders (99.9%; ALM43, Sumitomo Chemical Co. Ltd., Tokyo, Japan) in a range from 40 to 60 wt% were mixed with the SBCM glass frit by ball milling in ethanol for 12 h. The mixture was dried and then pressed uniaxially at ~80 MPa to form disk pellets with a diameter of 20 mm. The pellets were then sintered at 825–925 °C for 2 h at a heating rate of 2 °C/min.

### 2.2. Characterisation

The bulk density for the sintered samples was measured by the Archimedes method. The sintering shrinkage behaviour and thermal expansion coefficient (TEC) were measured using a dilatometer (DIL 402EP, Netzsch Instruments, Selb, Germany) with a heating rate of 5 °C/min in air. The crystalline phases were analysed by an X-ray diffractometer (D8 Advance, Bruker AXS, Karlsruhe, Germany) with Cu$K\alpha$ ($\lambda = 1.5405$ Å) radiation generated at 40 kV and 30 mA. The microstructures of the sintered samples were examined by scanning electron microscopy (SEM, S4800, Hitachi, Tokyo, Japan). The dielectric characteristics at 1 MHz were measured by an LCR metre (4285A, Agilent Co., Palo Alto, CA). The thermal diffusivity was measured using the laser-flash system (LFA457, Netzsch Instruments, Selb, Germany). Before measurement, sample surfaces were coated with a thin layer of colloidal graphite to increase the light absorption. The thermal conductivity ($k'$) of the sintered specimen was then determined using the formula $k' = \alpha C_p \rho$, where $\alpha$ is the thermal diffusivity, $C_p$ is the specific heat, and $\rho$ is the density. The flexural strength was measured using an electronic tensile testing machine (WDW-100, Changchun Research Institute of Testing Machines, Jilin, China) from three-point bend test with a span of 30 mm at a crosshead speed of 0.5 mm/min.

## 3. Results and discussion

### 3.1. Phase composition

The X-ray diffraction patterns of the samples containing 50 wt% $Al_2O_3$ recorded between 825 and 925 °C are shown in Fig. 1(a). The pre-existing $Al_2O_3$ was the main crystalline phase presented in the composites, whereas the additional crystalline phases, anorthite ($CaAl_2Si_2O_8$) and cordierite ($Mg_2Al_4Si_5O_{18}$), were found at all sintering temperatures. The formation of anorthite and cordierite might involve the reaction of $Al_2O_3$ filler with glass. Moreover, the anorthite phase increased with the increase in sintering temperature, which was the result of enhanced reaction between the glass and $Al_2O_3$ at higher sintering temperatures. However, it was notable that the cordierite phase could form at the relative low temperature (825 °C) and seemed to be stable with the increasing temperature.

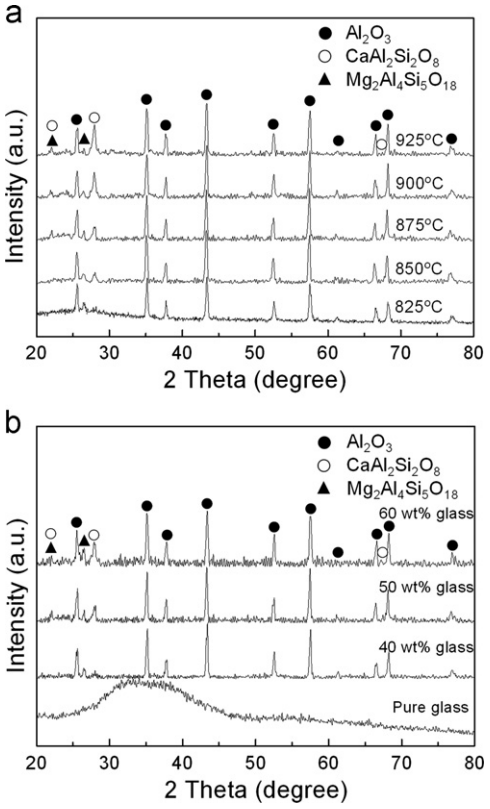


Fig. 1. X-ray diffraction patterns of glass/$Al_2O_3$ composites: (a) samples containing 50 wt% glass as a function of sintering temperature, and (b) samples containing different glass contents sintered at 875 °C.

The anorthite phase was also found to be a major phase as reported in the LTCC compositions composed of calcium borosilicate and $Al_2O_3$ filler [17]. It is well known that the densification of glass/ceramic can be classified as non-reactive, partially reactive, and completely reactive liquid phase sintering, depending on the reactivity between glass and ceramics [1]. Hence, in this study, the densification of SBCM glass/$Al_2O_3$ composites was considered to be partially reactive liquid sintering. The XRD patterns of the samples containing different contents of $Al_2O_3$ sintered at 875 °C are presented in Fig. 1(b). It was revealed that the starting glass sintering at 875 °C was basically composed of amorphous glassy phase, whereas $Al_2O_3$ was the main phase with a minor amount of anorthite and cordierite phase for the $Al_2O_3$-filled composites. Moreover, the relative intensity of the anorthite diffraction peaks strengthened gradually with increasing glass from 40 to 60 wt%. This result indicated that the increasing glass content enhanced the reaction between the glass and $Al_2O_3$. Generally, the chemical reaction between glass and ceramics can provide a good wetting condition [18], even though the higher weight per cent of glass will lead to the formation of secondary phase.

### 3.2. Sintering behaviour

The relative densities of the glass/$Al_2O_3$ composites as a function of sintering temperature from 825 to 925 °C are plotted in Fig. 2. The densities increased significantly with increasing sintering temperature for almost all the compositions. However, a saturated value was obtained for the samples with high glass content ( $\geq$ 50 wt%) at 875 °C and thereafter, relative densities slightly decreased, which was probably attributed to the boron-rich glass volatilization and a small amount of trapped porosity. This result indicated that the densification strongly depends on the sintering temperature and glass content. It was believed that the liquification of low-melt glass at the sintering temperature would facilitate particle rearrangement by the wetting of ceramic fillers and further densification was controlled by the viscosity of the glass-melt. The sintering temperature required to achieve high sintered density for the composites was thus reduced to ~875 °C.

In order to evaluate the sintering behaviour of the SBCM glass/$Al_2O_3$ composites, the dilatometric analysis was used to determine the shrinkage. Shrinkage behaviour of pure SBCM glass is presented for comparison (Fig. 3). The shrinkage data demonstrated that the glass densification started approximately from 615 °C (onset temperature) and finished till the glass started to melt. From the onset temperature to 900 °C, the viscous flow caused the significant shrinkage and gave a total shrinkage of ~18% for the glass. Additionally, the shrinkage rate of pure glass increased with temperature and reached its maximum value at 795 °C, and then decreased dramatically at higher temperatures. It was notable that the shrinkage rate once again increased until 883 °C, and thereafter it deceased with the further increase in heating temperature.

Fig. 4 shows the shrinkage curves measured at a heating rate of 10 °C/min for the samples with different concentrations of $Al_2O_3$ filler. It demonstrated that the onset of shrinkage took place at ~624 °C for all the samples and the onset temperature, which indicated the starting point of dimensional shrinkage, seemed to be independent on the content of glass. For 40 wt% glass-added sample (Fig. 4(a)), the linear shrinkage (~14.5%) was much smaller than that of the 50 wt% and 60 wt% glass-added samples (~17.6% for the former and ~17.9% for the latter, Fig. 4(b)–(c)). The results indicated that the more content of glass gave the greater linear shrinkage of the sample. It was notable that the linear shrinkage of 50 wt% and 60 wt% glass-added samples in the temperature range of 600–1000 °C was almost equal to that of the pure glass, which suggested that at least 50 wt% glass was needed to achieve densification. In addition, the highest densification rate of the sample with 40 wt% glass occurred at ~851 °C, which was much higher than that of the samples with 50 wt% and 60 wt% glass (831 °C and 816 °C, respectively). This result indicated that the sufficient glass was effective to accelerate the sintering of the composites. Hence, low temperature sintering could be achieved for the present glass/$Al_2O_3$ composites. It was noteworthy that the maximum densification rate of 50 wt% glass-added sample ($1.39 \times 10^{-3}$ °C$^{-1}$) was slightly higher than that of the

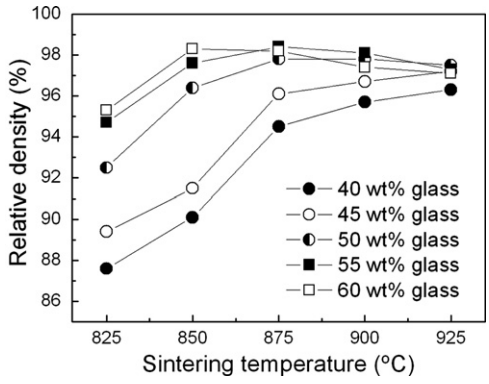


Fig. 2. Variation of relative density of glass added alumina as a function of temperature.

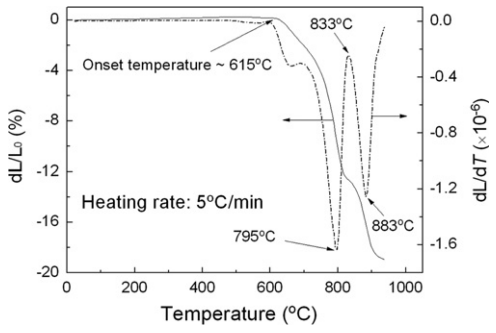


Fig. 3. Dilatometric curves (solid line, $dL/L_0$) and their derivatives (dash dot line, $dL/dT$) of SBCM glass.

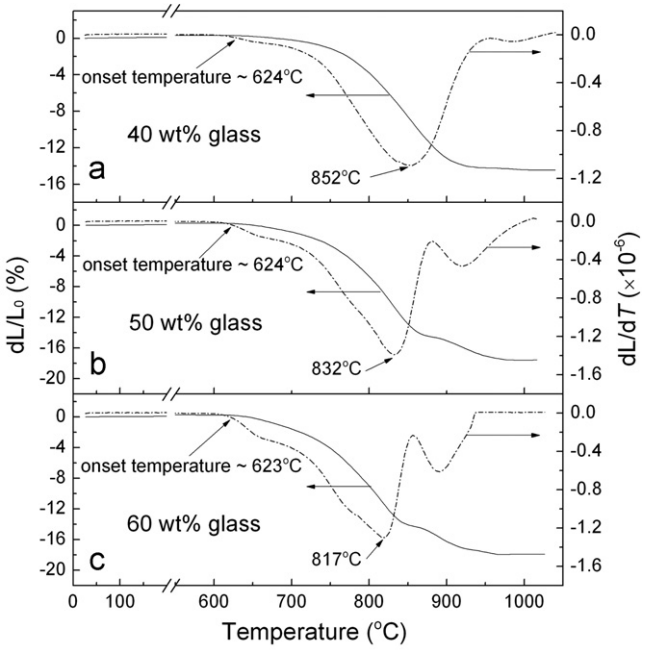


Fig. 4. Dilatometric curves (solid line, $dL/L_0$) and their derivatives (dash dot line, $dL/dT$) of SBCM glass/$Al_2O_3$ composites (a) 40 wt% glass, (b) 50 wt% glass, and (c) 60 wt% glass.

40 wt% ($1.10\times10^{-3}$ °C$^{-1}$) and 60 wt% ($1.29\times10^{-3}$ °C$^{-1}$) glass-added samples. It seemed that the maximum densification rate was independent of the glass content and the reason needed further investigation.

### 3.3. Microstructure

Fig. 5(a)–(d) demonstrates the SEM images of samples with 50 wt% glass sintered at different temperatures. An increase in relative density was evident between 825 and 925 °C and was consistent with the measured densities shown in Fig. 2. The sample sintered at 825 °C exhibited a porous microstructure (Fig. 5(a)), whereas the sample sintered at 875 °C showed typical characteristics of LTCC, where $Al_2O_3$ particles were distributed in the matrix of glass (Fig. 5(b)). It was notable that the $Al_2O_3$ was hardly found in the fracture section, which was attributed to the $Al_2O_3$ particles that were covered by a large amount of liquid phase (Fig. 5(c)). However, when the sintering temperature increased to 925 °C, the phenomenon of overheating occurred in 50 wt% glass-added sample with the increase in pores and consequently the decrease in the relative density (Fig. 5(d)). For 40% glass-added sample, the melting glass could not completely wet the $Al_2O_3$ particles, which resulted in a porous microstructure (Fig. 5(e)), whereas a dense microstructure was developed for the sample with 60% glass sintered at the same temperature (875 °C, Fig. 5(f)). It is understandable that the glass content in this system needs to be at least 50 wt% for densification. Otherwise, the fired structure is not sufficiently densified and is too porous. A typical schematic drawing of the compact glass/$Al_2O_3$ composites was shown in Fig. 6. $Al_2O_3$ particles distributed in the glass phase and the glass partially reacted with the filler to form new crystalline phase(s), which might affect the physical properties of the composites significantly.

### 3.4. Physical properties

A demand for high speed signal propagation in the communication system has resulted in major progress in the fields of large scale integration (LSIs) and circuit boards. To enable high speed switching of LSIs in a system, the circuit boards should have a low $\varepsilon_r$, thus allowing the signal to propagate with a shorter delay [1,7]. Table 1 shows the variation of $\varepsilon_r$ sintered at 850 °C and 875 °C for the glass/$Al_2O_3$ composites. $\varepsilon_r$ increased with the increasing glass content from 40 wt% to 50 wt%, presumably due to the increase in density. However, the $\varepsilon_r$ subsequently decreased as the glass content increased from 50 wt% to 60 wt%. The decrease in $\varepsilon_r$ for the samples with $>50$ wt% glass content was related to the low $\varepsilon_r$ for the SBCM glass. In general, the $\varepsilon_r$ of composites consisting of different phases can be evaluated with the empirical logarithmic mixture equation [19]:

$$\log\varepsilon_r = \sum V_i \log\varepsilon_i \quad (1)$$

where $V_i$ and $\varepsilon_i$ are the volume fraction and the permittivity, respectively, of phase i. $\varepsilon_r$ of SBCM glass was previously measured as ~6 by employing a noncrystallized sample. The $B_2O_3$- and $SiO_2$-rich glass are expected to have a low $\varepsilon_r$, due to the polarisability of $B^{3+}$(0.05 Å$^3$) and $Si^{4+}$(0.87 Å$^3$), which were much lower than those of $Ca^{2+}$ (3.16 Å$^3$) and $Mg^{2+}$ (1.32 Å$^3$) [20]. Thus, according to Eq. (1), the results in this study were reasonable because the $Al_2O_3$ had higher $\varepsilon_r$ compared with that of glass, anorthite and cordierite.

Another important dielectric parameter, the dielectric loss ($\tan\delta$) at 1 MHz was also evaluated with respect to various glass contents. Table 1 shows that all the composites possessed quite low dielectric loss (i.e. of the order of $10^{-3}$). The dielectric loss firstly decreased significantly with the increase of glass content, and then increased with the further increase in glass content. It is well known that the density (or porosity) of composites plays an important role in the dielectric loss variation. As discussed above, the 40 wt% content of glass was insufficient to achieve dense microstructure, and the dielectric loss therefore decreased when the glass content increased to 45 wt%. It is generally believed that the addition of glass deteriorates the dielectric loss of composite and the dielectric loss in glass may at least arise from a combination of migration losses and deformation losses. The migration losses are mainly caused by the movement of mobile ions ($Na^+$, $K^+$ in this study), while the deformation losses are dominated by the defect or deformation of the basic silicon oxide network [21]. Hence, when the glass content exceeded 50%, the higher

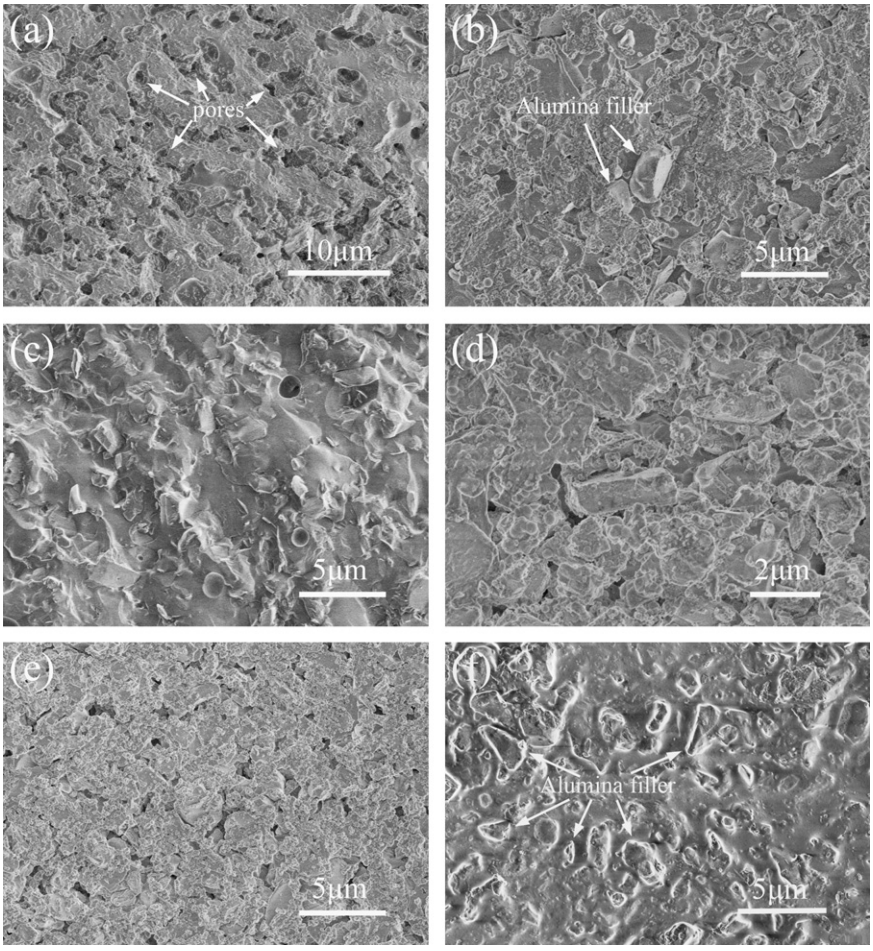


Fig. 5. SEM photographs of the glass added samples sintered at different temperatures: (a) 50 wt% glass sintered at 825 °C, (b) as-fired surface , (c) fracture section of 50 wt% glass sintered at 875 °C, (d) 50 wt% glass sintered at 925 °C, (e) 40 wt% glass sintered at 875 °C, and (f) 60 wt% glass sintered at 875 °C.

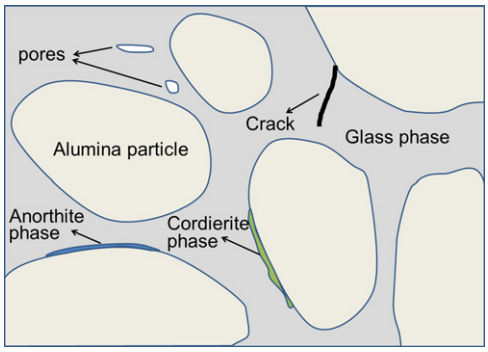


Fig. 6. The typical schematic drawing of the compact glass/$Al_2O_3$ composites.

dielectric loss was obtained since the dielectric loss was dominated by the amorphous glass phase. Even though the high level of glass content was able to enhance the sinterability, there was, however, a shortcoming concerning its high dielectric loss. Furthermore, the SBCM glass reacted with $Al_2O_3$ to form interface phase between $Al_2O_3$ and glass (Fig. 1), which is also considered to influence the dielectric properties of the composites. It was worth pointing out that the dielectric loss of the composites in this study was lower than most of the commercial LTCC substrate materials (Table 2), such as DuPont 951 (~0.0015), Ferro A6 (~0.002), Heraeus CT700 (~0.002), etc [1,22].

The thermal expansion coefficient (TEC), flexural strength and thermal conductivity of the samples containing different weight fractions of glass content are shown in Table 1. It was observed that the TEC of glass/$Al_2O_3$ composites in the range between 25 °C and 300 °C are 5–6 ppm/°C, which was close to that of Si (3.5 ppm/°C). Generally, TEC of the composites is dominated by the original raw material volume fractions. The SBCM glass, cordierite, and anorthite exhibit low TECs (3–5 ppm/°C, 2.5–3 ppm/°C [23], and 4.5 ppm/°C [24], respectively) compared with $Al_2O_3$ (6.5 ppm/°C) [25], and therefore the SBCM glass and the formation of cordierite and anorthite phase were believed to decrease the TEC of the samples. Moreover, the TEC decreased with the increase of glass content, since the amounts of glass and anorthite, which were responsible for decreasing thermal expansion, were increased (Fig. 1). The flexural strength of these samples was also determined in this study. It was evident

Table 1
Properties of glass/$Al_2O_3$ composites sintered at 850 °C and 875 °C for 2 h.

| Sintering temperature (°C) | Glass content (%) | $\varepsilon_r$ (1 MHz) | tan $\delta$ ($\times 10^{-3}$) (1 MHz) | TEC (ppm/°C) | Flexural strength (MPa) | Thermal conductivity (W/m °C) |
|---|---|---|---|---|---|---|
| 850 | 40 | 6.91 | 2.38 | 5.64 | 142 | – |
| | 45 | 7.05 | 1.77 | 5.59 | 163 | 3.56 |
| | 50 | 7.38 | 1.36 | 5.45 | 194 | 3.41 |
| | 55 | 7.31 | 1.51 | 5.26 | 179 | 3.37 |
| | 60 | 7.29 | 1.56 | 5.14 | 134 | 3.26 |
| 875 | 40 | 7.24 | 1.85 | 5.58 | 176 | 3.45 |
| | 45 | 7.48 | 1.52 | 5.54 | 202 | 3.69 |
| | 50 | 7.57 | 1.15 | 5.41 | 184 | 3.56 |
| | 55 | 7.35 | 1.52 | 5.21 | 165 | 3.31 |
| | 60 | 7.32 | 1.92 | 5.18 | 122 | 3.20 |

Table 2
Properties of relative commercial LTCC materials.

| Properties | DuPont 951 | Ferro A6 | Heraeus CT700 | This work |
|---|---|---|---|---|
| Sintering temperature (°C) | $<900$ | $<900$ | $<900$ | 875 |
| Permittivity, $\varepsilon_r$ | 7.8 | 5.9 | 7.0 | 7.57 |
| tan $\delta$ ($\times 10^{-3}$) | 1.5@1 kHz | 2@10 MHz | 2@1 kHz | 1.15@1 MHz |
| TEC (ppm/°C) | 5.8 | 7.0 | 6.7 | 5.41 |
| Flexural strength (MPa) | 320 | 130 | 240 | 184 |

from Table 1 that the flexural strength of glass/$Al_2O_3$ composites strongly depended on the glass content. Composites with 45 wt% glass sintered at 875 °C exhibited the highest flexural strength (202 MPa). The presence of $Al_2O_3$ particles could prevent the cracking growth in the glass/$Al_2O_3$ composites and enhance the mechanical strength. However, the excessive $Al_2O_3$ filler, such as 60 wt% $Al_2O_3$ in this study, would result in the development of porous microstructure, which could drastically damage the strength. Additionally, heat dissipation is a major problem in microelectronic devices and circuits [24]. In order to solve this problem, substrates with high thermal conductivity are required. As the $Al_2O_3$ content increased (thus glass decreased), the thermal conductivity of the composites also increased (Table 1). The $Al_2O_3$ filler seemed to improve the thermal conductivity of the composites as they acted as conducting channels with lower thermal resistance than the glass. In this study, the thermal conductivity of the present glass/$Al_2O_3$ composites was $\sim$3.5 W/m °C.

## 4. Conclusions

A glass/ceramic composite based on lead-free low melting glass ($SiO_2$–$B_2O_3$–MgO–CaO glass) with $Al_2O_3$ filler was fabricated at a sintering temperature of $\sim$875 °C. In the sintering process, the chemical reactions between glass and $Al_2O_3$ resulted in the appearance of anorthite and cordierite phases. The sintering behaviour, dielectric and thermal properties were sensitive to the amount of $Al_2O_3$ filler and sintering temperature. At least 50 wt% of SBCM glass content was required for sufficient densification. Optimum properties were exhibited for composites with 50 wt% glass and 50 wt% $Al_2O_3$ sintered at 875 °C with permittivity $\varepsilon_r$=7.3, tan $\delta$=1.15 $\times 10^{-3}$, TEC=5.41 ppm/°C, thermal conductivity=3.56 W/m °C and flexural strength=184 MPa. Therefore, the composite with 50 wt% glass could be a suitable candidate for low temperature cofired ceramic (LTCC), in the points of its low sintering temperature and outstanding physical properties.

## References

[1] M.T. Sebastian, H. Jantunen, Low loss dielectric materials for LTCC applications: a review, International Materials Reviews 53 (2008) 57–90.
[2] X.Y. Chen, S.X. Bai, W.J. Zhang, Low temperature sintering and microwave dielectric properties of $Bi_4B_2O_9$-added 0.25$CaTiO_3$–0.75($Li_{1/2}Nd_{1/2}$)$TiO_3$ ceramics, Journal of Alloys and Compounds 541 (2012) 132–136.
[3] H. Zhou, X. Liu, H. Wang, X. Chen, Low temperature cofiring and compatibility with silver electrode of ZnO–$SnO_2$–$TiO_2$–$Nb_2O_5$ ceramics with $BaCu(B_2O_5)$ addition, Ceramics International 38 (2012) 367–372.
[4] J. Honkamo, J. Hannu, H. Jantunen, M. Moilanen, W. Mielcarek, Microstructural and electrical properties of multicomponent varistor ceramics with PbO–ZnO–$B_2O_3$ glass addition, Journal of Electroceramics 18 (2007) 175–181.
[5] S. Ok, S. Heung, K. Soo, J. Guk, S. Kim, Low-temperature preparation and microwave dielectric properties of ZBS glass–$Al_2O_3$ composites, Ceramics International 35 (2009) 1271–1275.
[6] T. Takada, S. Nakao, M. Kojima, Y. Higuchi, Development, analysis, and application of a glass–alumina-based self-constrained sintering low-temperature cofired ceramic, International Journal of Applied Ceramic Technology 4 (2007) 398–405.

[7] A.A. El-Kheshen, Effect of alumina addition on properties of glass/ceramic composite, British Ceramic Transactions 102 (2003) 205–209.
[8] M. Hu, J. Xiong, H. Gu, Y. Chen, Y. Wang, Low temperature cofirable $Ca[(Li_{1/3}Nb_{2/3})_{0.95}Zr_{0.15}]O_{3+\delta}$ microwave dielectric ceramic with $ZnO–B_2O_3–SiO_2$ frit, Ceramics Internaional 38 (2012) 3175–3183.
[9] K.P. Surendran, P. Mohanan, M.T. Sebastian, The effect of glass additives on the microwave dielectric properties of $Ba(Mg_{1/3}Ta_{2/3})O_3$ ceramics, Journal of Solid State Chemistry 177 (2004) 4031–4046.
[10] J.-M. Wu, H.-L. Huang, Microwave properties of zinc, barium and lead borosilicate glasses, Journal of Non-crystalline Solids 260 (1999) 116–124.
[11] M.-Z. Jhou, J.-H. Jean, Low-fire processing of microwave $BaTi_4O_9$ dielectric with $BaO–ZnO–B_2O_3$ glass, Journal of the American Ceramic Society 89 (2006) 786–791.
[12] J.H. Park, Y.J. Choi, J.G. Park, Low-fire dielectric compositions with permittivity 20–60 for LTCC applications, Materials Chemistry and Physics 88 (2004) 308–312.
[13] C.-S. Chen, C.-C. Chou, W.-J. Shih, K.-S. Liu, C.-S. Chen, I.N. Lin, Microwave dielectric properties of glass–ceramic composites for low temperature co-firable ceramics, Materials Chemistry and Physics 79 (2003) 129–134.
[14] C.-C. Chiang, S.-F. Wang, Y.-R. Wang, Y.-F. Hsu, Characterizations of $CaO–B_2O_3–SiO_2$ glass–ceramics: thermal and electrical properties, Journal of Alloys and Compounds 461 (2008) 612–616.
[15] A. Yang, H. Lin, L. Luo, W. Chen, Microwave dielectric properties of low temperature cofired glass-ceramic based on $B_2O_3–La_2O_3–MgO–TiO_2$ glass with $La(Mg_{0.5}Ti_{0.5})O_3$ ceramics, Japanese Journal of Applied Physics 45 (2006) 1698–1701.
[16] Y. Imanaka, Multilayered Low Temperature Cofired Ceramics (LTCC) Technology, Springer, Berlin, 2005.
[17] Y.J. Seo, J.H. Jung, Y.S. Cho, J.C. Kim, N.K. Kang, Influences of particle size of alumina filler in an LTCC system, Journal of the American Ceramic Society 90 (2007) 649–652.
[18] J.-H. Jean, S.-C. Lin, Low-fire processing of $ZrO_2–SnO_2–TiO_2$ ceramics, Journal of the American Ceramic Society 83 (2000) 1417–1422.
[19] C.-L. Lo, J.-G. Duh, B.-S. Chiou, W.-H. Lee, Low-temperature sintering and microwave dielectric properties of anorthite-based glass–ceramics, Journal of the American Ceramic Society 85 (2002) 2230–2235.
[20] R.D. Shannon, Dielectric polarizabilities of ions in oxides and fluorides, Journal of Applied Physics 73 (1993) 348–366.
[21] T. Takada, S.F. Wang, S. Yoshikawa, S.J. Jang, R.E. Newnham, Effect of glass additions on $BaO–TiO_2–WO_3$ microwave ceramics, Journal of the American Ceramic Society 77 (1994) 1909–1916.
[22] H. Jantunen, A Novel Low Temperature Co-Firing Ceramic (LTCC) Material for Telecommunication Devices, Oulu University Press, Oulu, 2001, pp. 15–44.
[23] C.A. Harper, Handbook of Ceramics, Glasses, and Diamonds, McGraw-Hill, New York, 2001.
[24] G.-H. Chen, L.-J. Tang, J. Cheng, M.-H. Jiang, Synthesis and characterization of CBS glass/ceramic composites for LTCC application, Journal of Alloys and Compounds 478 (2009) 858–862.
[25] C. Janardhanan, D. Thomas, G. Subodh, S. Harshan, J. Philip, M.T. Sebastian, Microwave dielectric properties of flexible butyl rubber–strontium cerium titanate composites, Journal of Applied Polymer Science 124 (2012) 3246–3433.